PAPER

Check for updates

Development of continuous spatially distributed diafiltration unit operations†

Zoheb Khan,‡[abd] Xiaoyan Long,‡[ad] Eoin Casey, [iD][a]
Denis Dowling[c] and Steven Ferguson [iD] *[abde]

The objective of this study is to develop an operation that can conduct separations based on diafiltration using semipermeable nanofiltration or ultrafiltration membranes in a fully continuous manner in a single stage configuration. To this end, a continuous spatially distributed diafiltration (CSDD) operation is developed herein that aims to conduct continuous single stage diafiltration in a manner that would yield equivalent or better purification efficiency than both batch and incumbent single stage continuous diafiltration configurations. To achieve this goal, a diafiltration solvent is introduced spatially across the membrane unit in a highly uniform manner, with the flow guided by a range of 3D-printed static mixers, developed by CFD informed design, to increase localized mixing of retentate and diavolume flows or displacement effects within the membrane channel. Static mixers were 3D-printed using titanium and polyether ether ketone (PEEK) providing high pressure and chemical compatibility, suited for intensive continuous processes. Ibuprofen was selected as a model active pharmaceutical ingredient (API) with methanol and ethanol used in model impurity removal and solvent swap scenarios with an organic solvent nanofiltration membrane used to selectively retain ibuprofen. Significant improvements in solvent consumption and yield were realized with both CSDD based purification and solvent exchange operations compared to batch diafiltration. As such, CSDD may present an attractive intermediate purification and solvent swap operation for telescoped flow chemical and continuous processing applications, in addition to a highly compatible platform for use in small scale automated flow-based experimentation.

1. Introduction

Flow chemistry and continuous processes have seen significant uptake in process development and intensified manufacturing of complex high value but low volume fine chemical, pharmaceutical and biopharmaceutical products.[1–5] However, continuous work-up and purification operations for continuous manufacturing require further development to facilitate the significant level of purification and stream adjustment in multistep routes that batch synthesis

traditionally offers in the production of these classes of chemical products.[6–8] Continuous manufacturing requires integration into a complete multi-step continuous process to maximize process intensification. As such, a wider range of possible unit operations and design strategies have been explored to facilitate integrated processes.[9] The development of flow chemical processes has coincided with significant developments in the field of organic solvent nanofiltration, where membrane compositions and operating strategies compatible with a wide array of chemical systems have been demonstrated.[10,11] Continuous OSN (organic solvent nanofiltration) operations in conjunction with flow chemical processes have been used to concentrate and purify process streams,[12,13] remove and recycle catalysts,[13,14] and conduct solvent swaps.[15] In addition, iterative liquid phase membrane enabled approaches have been used in the synthesis of larger molecular weight compounds such as peptides, RNAs and polymers.[11,16–18] Continuous OSN separation has also been utilized in hybrid approaches to enhance adsorption,[19] chromatography,[20] and crystallization[21] operations to conduct flow-based purification. Significant numerical optimization of multi-step configurations in continuous nanofiltration based separation with existing membrane module designs has also

[a] *School of Chemical and Bioprocess Engineering, University College Dublin, Belfield, Dublin 4, Ireland. E-mail: steven.ferguson@ucd.ie*
[b] *I-form, the SFI Research Centre for Advanced Manufacturing, School of Chemical and Bioprocess Engineering, University College Dublin, Belfield, Dublin 4, Ireland*
[c] *I-form, the SFI Research Centre for Advanced Manufacturing, School of Mechanical and Materials Engineering, University College Dublin, Belfield, Dublin 4, Ireland*
[d] *SSPC, the SFI Research Centre for Pharmaceuticals, School of Chemical and Bioprocess Engineering, University College Dublin, Belfield, Dublin 4, Ireland*
[e] *National Institute for Bioprocess Research and Training, 24 Foster's Ave, Belfield, Blackrock, Co. Dublin, A94 X099, Ireland*
† Electronic supplementary information (ESI) available. See DOI: https://doi.org/10.1039/d3re00013c
‡ These authors contributed equally to this study.

This journal is © The Royal Society of Chemistry 2023

React. Chem. Eng., 2023, **8**, 1785–1798 | 1785

been conducted.[22,23] As such, continuous nanofiltration operations now present an attractive single-phase operation for purification and stream adjustment within flow chemical and continuous chemical processes in both research and commercial applications.

Continuous diafiltration is typically achieved either by using a cascade of counter current contacting membrane modules or using a single pass tangential flow filtration (SPTFF) system, which is straightforward and implements continuous filtration by a single pass of the solution over a relatively increased permeation area and residence time as opposed to a conventional tangential flow filtration (TFF).[24] However, to achieve an acceptable level of solute reduction with an SPTFF, an impractical ratio of buffer flow to feed flow rates is required, while the number of pumps required and equipment complexity present disadvantages to counter current contacting membrane modules in a cascade configuration for some applications.[25]

A single-pass tangential flow filtration (SPTFF) process for protein concentration, operating in a continuous mode, was tested against the conventional TFF (tangential flow filtration).[26] The SPTFF modules consist of internally staged T-series cassettes for creating longer flow paths and having a smaller equipment footprint that result in significantly higher conversion in one pass. With SPTFF, the feed and retentate flow rates were set through flow ratio control, attaining the desired concentration factor and final formulation instantly, and minimizing the number of pump passes to only one. Single-pass tangential flow filtration has been demonstrated as an inline concentration step to clarify cell culture harvest for six different biopharmaceutical products.[27]

An alternative two membrane design of a single piece diafiltration equipment has also been proposed for protein solutions.[28] The device was composed of a 3D-printed single pass diafiltration (SPDF) module containing two commercial ultrafiltration membranes through which the flow directions of the DF buffer and the permeate were cyclically reversed while the feed solution was continuously pumped through the module. The flow reversal assisted in a backflush which reduced the concentration polarization layer to acceptable limits. The configuration was able to achieve a buffer exchange of up to 99.9% without the need for coupling several modules or intermediate dilution and mixing steps, but only 50% of the membrane area is utilized for separation at a given point in time.

Diafiltration is often considered to be an inherently batch process, the feed continuously cycles through the membrane, and the buffer solvent is fed at the same rate as the permeate flow out rate of the system. The work in the field of continuous diafiltration primarily focuses on SPTFF or cascades; however, even implementing the SPTFF with inline mixing would require a prohibitive buffer to feed flow rates.[29,30] In this study, significant work, with the aid of computational fluid dynamics (CFD), has been conducted to assess the performance of industrially relevant static inline

mixers in membrane channels, and this builds on the significant existing literature studying static mixer performance in pipe and channel flows.[31] The contemporary numerical schemes and modeling approaches have been discussed along with the parameters to estimate the performance characteristics. For example, a modified design of the Kenics static mixer is analysed, featuring gaps between the mixing elements, which can achieve the same level of mixing as the conventional design but with fewer mixing elements and a substantially lower pressure drop.[32] CFD modeling has been used in several membrane systems to study the influence of turbulence promoters and static mixers to enhance the permeate flux or mitigate fouling on the membrane surface.[33] Local parameters such as stream function, velocity, static pressure, wall shear stress, turbulent kinetic energy, and turbulent dissipation energy on the membrane surface are essential to making informed decisions on the influence of the promoters.[31,34–38] The current work uses industrially relevant static mixers *i.e.* Kenics and SMX and its variants to investigate the impact of flow characteristics on the CSDD operation in the membrane channel.

In the present work, a novel single pass diafiltration operation, continuous spatially distributed diafiltration (CSDD), is proposed and demonstrated. To achieve this goal, a diafiltration solvent is introduced spatially in a highly uniform manner with the flow guided by a range of 3D-printed mixers developed by CFD informed design to increase localized mixing of retentate and diavolume flows or displacement effects within the channel. Static mixers were 3D-printed using titanium and polyether ether ketone (PEEK) providing high pressure and chemical compatibility,[39] suited for intensive continuous processes with performance evaluated using a model pharmaceutical system.

2. Continuous spatially distributed diafiltration mechanisms of operation

As outlined in the introduction, single stage diafiltration operations face a dilemma in their operation as currently constituted.[25] If a diafiltration medium is added in a single addition followed by single stage concentration, the buffer requirements to enable significant separation are prohibitive. For purification to a $1:1\,000\,000$ from an equimolar starting point, $10\,000$ diavolumes would be required, in a single addition continuous diafiltration compared to approximately 14 diavolumes in batch operation under the assumption of perfect membrane performance.[25] Continuous cascades can reduce the diavolume requirements for this separation below those required in batch operation; for example, the equivalent separation can be made by 9.2 diavolumes in a 3-stage counter-current cascade. However, cascade configurations in membrane systems require $n + 1$ pumps per n-stages utilized which often discourages the use of membrane cascades in chemical and biochemical processes with intermediate pumps particularly constraining in small

scale applications. For this reason, many attempts to utilize membranes in continuous downstream biopharmaceutical separation for example have opted for the use of parallel batch systems where diafiltration based membrane separations are required.

Continuous spatially distributed diafiltration is investigated herein as an attempt to develop a single stage simplified alternative to cascades or parallel batch operation. In the proposed process, diafiltration is spatially distributed over the membrane channel, with the goal of reaching or exceeding the performance of batch diafiltration in terms of purity *versus* the number of diavolumes utilized. For non-ideal membranes where the product is not perfectly retained (*i.e.* $Re_j < 1.0$), this may also manifest as an equivalent or improved product yield at a targeted level of purity. Such cases will be particularly useful in separations for developing flow chemical approaches, due to selectivity limitations of membrane separations, which motivated the choice of example separation used in this study (section 3).

To aid in the discussion of the results in section 5, idealized conceptual models of the extremes of mixedness given the names continuous spatially distributed diafiltration (CS2D) and continuous spatially distributed displacement diafiltration (CS3D) are introduced here to facilitate a qualitative discussion of the mechanism of separation within real continuous spatially distributed diafiltration systems and in the interpretation of the results. Idealized schematic and analogous batch operating schemes of operation for idealized CS2D and CS3D operations are shown in Fig. 1. In Fig. 1(b), the idealized CS2D operation is shown; in this case, the feed is pumped continuously into a rectangular channel and flows across the channel from left to right. A diafiltration buffer/ solvent is continuously pumped into the rig, such that it is

uniformly spatially distributed along and across the channel. The process flow rates are operated such that the permeate flow rate and the diafiltration flow rate are the same, resulting in no net dilution or concentration. In such a scenario, a mixing profile like an idealized plug flow is desired within the channel, with no velocity gradient along the horizontal axis or back or forward mixing towards the inlet or outlet. Ideally, perfect mixing between the perpendicular flows of diavolumes and crossflow at every point along the membrane channel should occur. Where such conditions can be approximated, idealized CS2D can be achieved and thought of as a constant volume batch diafiltration shown in Fig. 1(a) but occurring over the length of the channel rather than with respect to time. In this idealized case, performance with respect to impurity removal *versus* the number of diavolumes should be the same as the performance of a constant volume batch diafiltration. While such idealized mixing is not possible to achieve, it can be closely approximated by many highly turbulent flows or segmented mixing elements, in an analogous manner to CSTRs in series approximating the performance of a plug flow reactor, but for diafiltration operations. This provided the basis for the design of the CS2D mixers shown in the ESI.†

Fig. 1(d) shows a schematic of the idealized CS3D operation and the equivalent batch operating procedure (Fig. 1(c)). As in the case of the ideal CS2D operation, there is no back-mixing left to right along the length of the channel and an idealized flow from the inlet to the outlet is envisioned. However, in contrast to the ideal CS2D operation, the CS3D operation aims to have no mixing of the diafiltration solvent and the crossflow stream. In this mode of spatially distributed diafiltration, the secondary
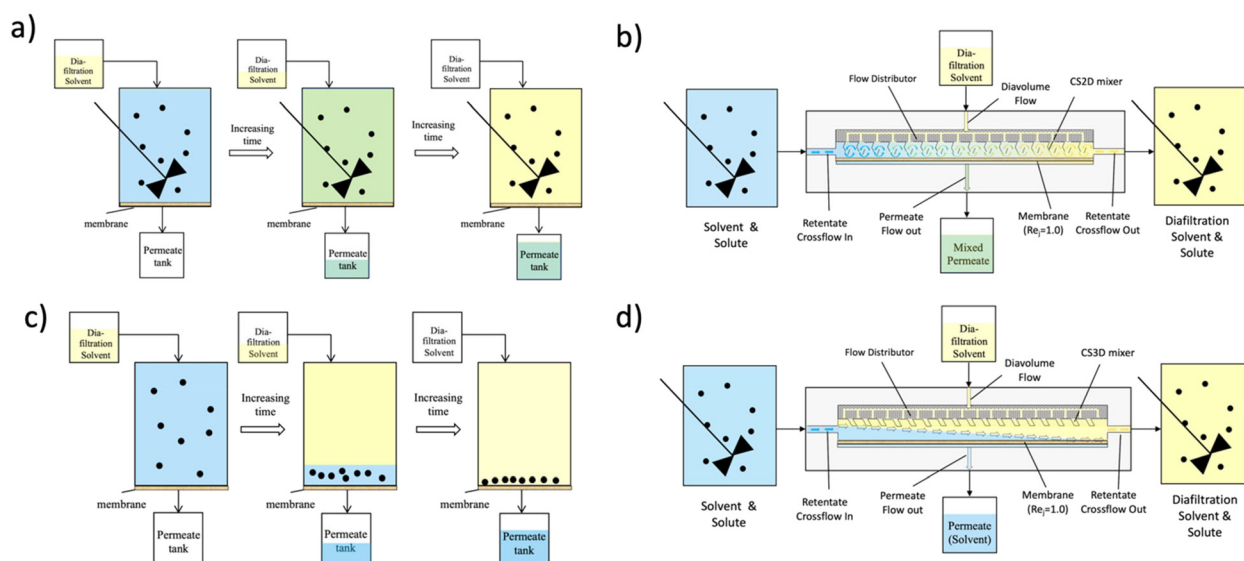

Fig. 1 Conceptual illustration of idealized (a) constant volume batch diafiltration in a well-mixed batch reactor; (b) continuous spatially distributed diafiltration (CS2D) schematic (constant volume operation); (c) constant volume batch displacement diafiltration in an unmixed batch reactor; (d) continuous spatially distributed displacement diafiltration (CS3D) schematic (constant volume operation). Diafiltration and permeate tanks are not to scale.

This journal is © The Royal Society of Chemistry 2023

React. Chem. Eng., 2023, **8**, 1785–1798 | **1787**

diafiltration flow attempts to displace the primary flow moving along the length of the membrane channel convectively towards the membrane wall. While the primary solvent filters through the membrane and gets displaced, the solute moves over into the secondary displacing solvent as it is retained by the membrane. Ideally, the secondary solvent replicates the action of a piston pump pushing the primary solvent through the membrane, as the overall net flow moves from left to right across the channel with an ideal flat flow velocity profile.

If such a flow could be realized in principle when a flow rate ratio of feed to diafiltration solvent flow of 1 : 1 is used, 100% removal of primary solvent or impurities should be achievable with only a single diavolume being needed for an ideal membrane. However, in achieving this high efficiency for theoretical purification efficiency, an inherent disadvantage of this mode of operation is the formation of a polarized solute layer on the membrane surface, which likely under real conditions leads to significant reduction in flux or precipitation on the membrane surface making the unit inoperable. The design and testing of mixers attempting to allow a real CS3D mode of diafiltration operation to be investigated are shown in the ESI.†

The equivalent idealized batch operation to CS3D (Fig. 1c) more clearly illustrates the effect of displacement in diafiltration. In this schematic, a diafiltration solution is carefully added so as to avoid the mixing of the diafiltration solvent and feed solvent in an unmixed batch vessel with the membrane at the bottom. As an additional solvent is added, increased pressure in the closed system pushes the feed solvent out through the membrane, with the solute retained and concentrated at the membrane. If in the schematic experiment the addition of diafiltration solution is conducted over a sufficiently short timescale where diffusion between the layer of the diafiltration solvent and feed solvent and

solute is negligible, a perfect separation where one solvent displaces the other is achieved with the addition of 1 diavolume of solvent resulting in 100% removal of feed solvent which is collected in the permeate tank as a purified solvent where all solute is retained.

Fig. 2 shows a schematic diagram of impurity concentration *versus* the number of diavolumes for ideal CS2D which will have equivalent performance to batch diafiltration. As would be expected, it takes the form of an exponential washout curve. An ideal CS3D operation will show linear displacement of impurity over the course of 1 diavolume flow rate under ideal conditions. The behaviour of real mixers will fall somewhere between these two extremes in practice. It should be noted that ideal displacement diafiltration type flow patterns are likely to result in a decrease in flux, and propensity for membrane fouling so the goal in design is to find a balance between these mixing profiles rather than to maximize displacement effects. Furthermore, where significant back mixing towards the feed or short-circuiting or diafiltration flows occurs, less favourable separation performance may be observed outside of the shaded area between the extremes of no/perfect mixing of crossflow and diavolume flows in the direction perpendicular to the membrane. In practice, a perfect flat velocity profile across the channel is also an idealized assumption but in principle such flows can be approximated even under laminar conditions *via* the use of static mixers in conventional pipe and channel flows.[30] Where permeate and diavolume flow rates are not equal, a net concentration or dilution will take place across the channel which may improve or decrease the diafiltration efficiency respectively as would be anticipated in equivalent batch operation. However, this may encourage local net flows to the interface or bypass flows taking the operating region outside of the conceptual (blue) operating region outlined in Fig. 2. This conceptual model was used to inform initial mixer design efforts, which aimed to develop real continuous spatially distributed diafiltration mixers (section 4) to both meet and exceed the separation efficiency of batch diafiltration shown in section 5.

3. Experimental

3.1 Membrane test module and 3D-printed CS2D and CS3D mixer construction

The CS2D and CS3D experiments were carried out in a custom designed membrane assembly unit fabricated with stainless steel. The membrane unit can house a variety of mixer designs which can be chosen based on the process and flow behaviour requirements. The membrane module channel was 30 mm wide, 55 mm long and 1 mm in height. Mixer designs were informed *via* CFD and the static mixer literature as outlined in section 1. Additional information concerning the membrane rig and individual mixer design and fabrication are shown in the ESI† of this article. The mixers were 3D printed with polyether ether ketone (PEEK)
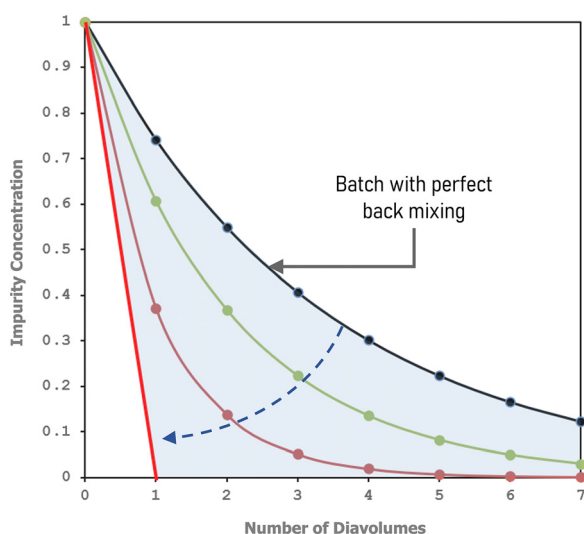

Fig. 2 Schematic diagram of impurity concentration as a function of the number of diavolumes for an ideal CS2D performance, ideal CS3D performance and intermediate real CSDD performance.

1788 | *React. Chem. Eng.*, 2023, **8**, 1785–1798

This journal is © The Royal Society of Chemistry 2023

using an APIUM M220 owing to its compatibility with a wide range of solvents and its structural stability at high operating pressures.[39] The designs were relatively simple and allowed a straight through flow with the buffer solution impinging at different angles on the membrane surface. Mixers with mixing element designs involving curved surfaces and acute printing angles were fabricated with powder bed titanium printing (DMP Flex 350s). Dual overhangs within the mixer designs were enabled by designing the mixers with modifications, to provide structural stability and ease of printing while maintaining desired geometry and hence mixing characteristics, as outlined in the ESI.†

3.2 Experimental materials

An ibuprofen (202 Da)–ethanol (46.7 Da) mixture (1% w/v ibuprofen, 10% v/v ethanol) was prepared in a methanol solution. A commercially available modified polyamide membrane: DuraMem150 (Evonik Resource Efficiency GmbH, high performance polymers, Paul-Baumann- Strasse 145 772 Marl, Germany) with a molecular weight cut-off (MWCO) of 150 Da was used for all experiments to study the performance of separation and solvent swap using different mixer configurations. The membrane area available within each experiment was (5.5 cm × 3cm) 16.5 cm^2. Stability and permeability tests were conducted prior to and between experimental runs to ensure that consistent membrane performance was maintained. Ethanol and methanol (Fisher Scientific Ireland Ltd.) used were of analytical reagent grade and HPLC grade respectively, with a purity of ≥99.8%.

3.3 Analytical methods

The ibuprofen concentration in the retentate was measured using a UV-1800 high-resolution spectrophotometer from Shimadzu and the ethanol purity in the permeate stream was measured using a Nexis GC-2030 gas chromatograph from Shimadzu (column: SH-Rxi-5 ms). Ibuprofen shows notable spectral adsorption in the lower UV region which was measured through UV spectroscopy (UV-1800, Shimadzu) and used in determining its concentration in the retentate and permeate streams. GC samples were diluted with a mixture of toluene and anisole. The ratio of ethanol and anisole peak areas was applied to the calibration curve:

$$Yield = \frac{C_{ibuprofen,0}}{C_{ibuprofen,n}} \tag{1}$$

$$Purity = \frac{C_{ibuprofen,n}}{C_{ibuprofen,n} + C_{ethanol,n}} \tag{2}$$

where $C_{ibuprofen,0}$ is the concentration of ibuprofen at the start of the diafiltration (mg mL^{-1}), $C_{ibuprofen,n}$ is the concentration of solute ibuprofen after the nth number of diavolumes (mg mL^{-1}) and $C_{ethanol,n}$ is the concentration of ethanol after the nth number of diavolumes (mg mL^{-1}). For the continuous operation modes, the number of diavolumes is the ratio of the buffer flow rate and feed flow rate. Product samples are

collected from the retentate stream in this system. The purity and yield are calculated from eqn (3) and (4):

$$Purity = \frac{C_{ibuprofen,r}}{C_{ibuprofen,r} + C_{ethanol,r}} \tag{3}$$

$$Yield = \frac{C_{ibuprofen,r}}{C_{ibuprofen,f}} \times \frac{Q_r}{Q_f} \tag{4}$$

where $C_{iburpofen,r}$ and $C_{ethanol,r}$ are the ibuprofen and ethanol concentrations in the retentate stream (mg mL^{-1}) and $C_{ibuprofen,f}$ is the ibuprofen concentration in the feed vessel (mg mL^{-1}). Q_r and Q_f are the retentate and feed flow rates, respectively (mL min^{-1}).

3.4 Experimental set up and procedure

A diafiltration buffer solution was introduced perpendicular to the feed flow and is uniformly distributed across the channel volume, with a porous steel filter which is also utilized to support the membrane on the opposite side of the channel (Fig. 3). Images of the fabricated mixers and visualization of flow patterns are shown in the ESI† of this article (ESI† Fig. S3 and S4).

The inlet flows were controlled using a dual-headed high-pressure pump (LD series, SSI). The pumps were primed with methanol before a set of experiments to ensure the longevity of the piston rings and to maintain the purity of the studied system. The diafiltration experiments were carried out at a constant transmembrane pressure of 55 bar at room temperature. The pressure in the system was monitored with a 0–60 bar pressure sensor (Gems Sensor and Controls) and recorded by a PicoLog 1012 data logger (Pico Technology). In order to provide time for membrane performance to stabilize under experimental conditions, the retentate and permeate outlets are fully recycled to the feed tank for 1 hour at 5 mL min^{-1} and 55 bar before commencing with batch diafiltration runs. In all experiments stable steady state performance was confirmed *via* online pressure and UV measurements in addition to measurement of retentate and permeate flow rates *via* sampling.
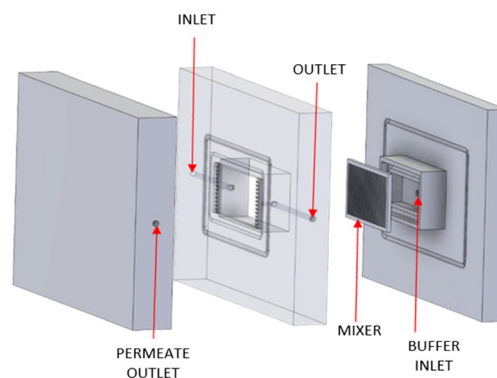

Fig. 3 Schematic of the membrane assembly unit machined. Different 3D printed mixers can be inserted within the assembly for testing and characterization.

This journal is © The Royal Society of Chemistry 2023

React. Chem. Eng., 2023, **8**, 1785–1798 | **1789**

In the continuous diafiltration experiments, the buffer stream was pumped through the buffer inlet (Fig. 3), with this flow meeting the retentate crossflow, which entered at the inlet and exited at the outlet (Fig. 3) orthogonally, mixing with and displacing the passing cross flow. The permeate passes through the membrane which sits on a porous metal support within the permeate outlet collection section (Fig. 3) exiting through the permeate outlet. Each run was confirmed to reach a stable steady state at 55 bar transmembrane pressure using an inline pressure transducer and UV absorbance measurements. For all experiments, permeate and retentate flow rates were also measured *via* sampling to confirm steady state operation. These values were used to calculate the flux values as shown in Fig. 6 and 8. Minor adjustment to the back pressure regulator, and pumps controlling feed and diafiltration flow rates were made to ensure operation at 55 bar transmembrane pressure and that permeate and diafiltration flow rates were equal thus establishing constant volume diafiltration conditions in all runs. For example, for the SMX experiments as shown in Fig. 6, retentate flow rates are 0.26 ml min^{-1}, 0.14 ml min^{-1}, 0.10 ml min^{-1}, 0.80 ml min^{-1} at 1 to 4 relative diavolumes/ permeate flow rates, respectively. The real time absorbance of ibuprofen in the retentate stream was recorded with flow through UV spectroscopy at a wavelength of 263 nm and three sets of samples were collected from the permeate and retentate after the absorbance reached steady state.

For the solvent swap experiments, ibuprofen was selected as an API dissolved in methanol exchanged with ethanol and acetonitrile. 1%, 0.5% and 0.2% w/v ibuprofen (206 Da)–methanol (32.04 Da) mixtures are prepared for solvent swap applications in constant volume batch diafiltration, CS2D and CS3D operation modes. Ethanol (EtOH, 46.07 Da), methanol (MeOH, 32.04 Da) and acetonitrile (MeCN 41.05 Da) are purchased from Fisher Scientific Ireland Ltd. with ≥99.8% purity. 10 g, 5 g, and 2 g ibuprofen (KemproTec) are weighted and dissolved in 1 L methanol as the diafiltration feed solution. Toluene and anisole were purchased from Fischer Scientific Ireland Ltd. for methanol, ethanol and acetonitrile concentration measurements in GC analysis.
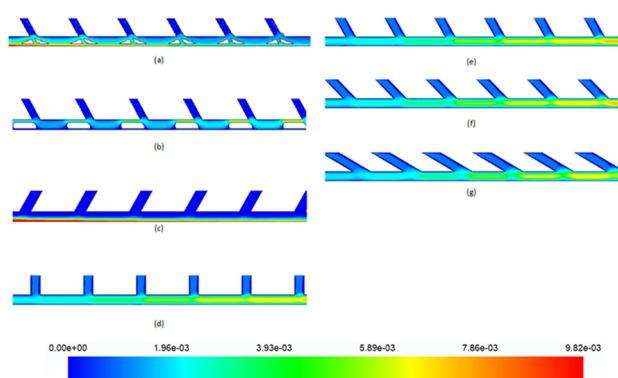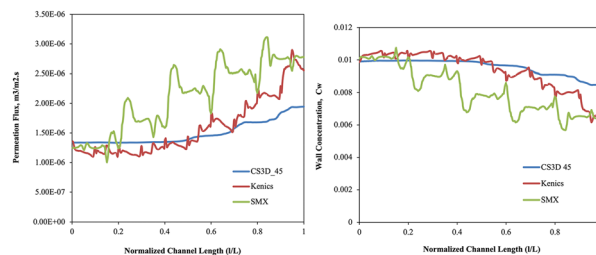

Fig. 5 Comparison of CS3D and CS2D geometries for the (left) permeation flux and (right) wall concentration against the normalized channel length.

4. CFD simulation informed mixer design

4.1 CFD simulation strategy

Investigation of the flow dynamics in relation to the polarization concentration in membrane channels with CFD has emerged since the late 1990s.[29] Along with the numerical computation, implementation of experiments for predicting parameters and validation is of crucial necessity to avoid dependence on mass transfer modeling of semi-empirical correlations. A two-dimensional rectangular geometry is generated using the commercial CFD package ANSYS (Fig. S21-ESI†). The solution domain was identical to the experimental setup by Ahmed and Lau[40] *i.e.* ($l \times h$) 255 mm × 1 mm, and was used to verify the modeling assumptions and permeation flux model used in this study. A detailed description of the CFD modeling approach used in this study can be found in section 4 of the ESI† of this manuscript.

4.2 Flow visualization and analysis of CS3D geometries

CS3D mixers aim to enable displacement effects as discussed in section 2 to improve diafiltration solvent usuage efficiency. As outlined, the theoretical limit for this approach will be complete purification with a feed to diavolume flow ratio of one (section 2). However, this limit is unlikely to be closely approximated due to difficulties in completely preventing mixing between impinging diavolumes and cross flows, and furthermore at idealized displacement, diafiltration is approached, and concentration polarization at the membrane retentate interface is likely to cause a reduction flux and fouling.

Fig. 4 shows the velocity contours for the different geometries simulated. The primary flow moves along the positive *x*-axis (*i.e.* left to right) and the dilutant enters along the negative *y*-axis (*i.e.* from top to bottom) from the entry points built over the membrane channel and exit collection and permeate outlet below the membrane. The obstacles built in the way of the primary flow split the flow and redirect the streams to mix with the dilutant flow entering orthogonally and focus the another part of the split flow along the membrane surface.

Simple two-dimensional geometries were simulated to test and visualize the flow in the presence of the mixer. The

Fig. 4 Velocity vector and contour profiles for CS3D mixer geometries. Geometries simulated: (a) CS2D-Tri. (b) CS2D-Rect. (c) CS3D-120. (d) CS3D-90. (e) CS3D-60. (f) CS3D-45. (g) CS3D-30.

1790 | *React. Chem. Eng.*, 2023, **8**, 1785–1798

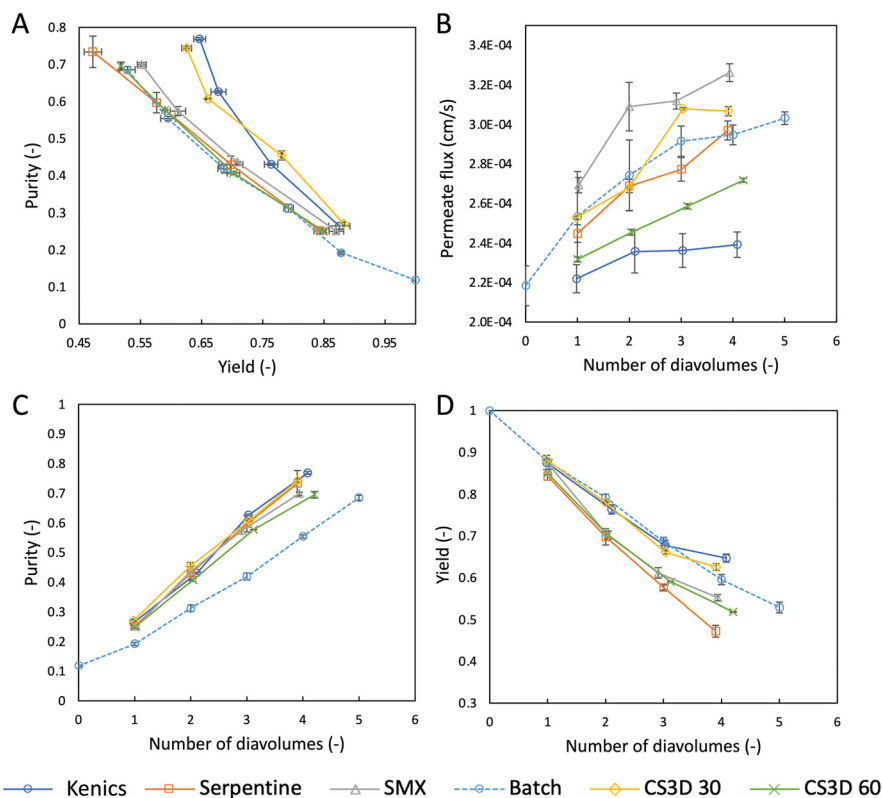This journal is © The Royal Society of Chemistry 2023

Fig. 6 Performance analysis for CSDD type mixers: (A) purity as a function yield achieved, (B) permeate flux (cm s^{-1}) as a function diavolumes utilized, (C) purity as a function of the number of diavolumes utilized, and (D) yield as a function of the number of diavolumes utilized. Mean values are calculated from independent steady state attaining experiments plotted with standard error of the mean (n = 3).

dilutant is introduced at varying angles to the primary feed flow axis. The inlet angles are varied as 30°, 45°, 60° and 90° and are characteristic of the CS3D geometries. The various angles were chosen to cover the range at which the buffer solution could enter the channel. The angles ranged from 30 to 120 degrees. With the highly obtuse angled inlets, there is severe backflow which is against the objective. The acute

Fig. 7 Solute concentration build-up along the membrane channel length.

angled vanes allowed the buffer feed to displace and push the feed along the flow direction, thus preventing any backflow against the feed flow direction and displacing the feed solution. The 90° angled vane was not adding any displacement effects with a slight backflow at the point of impingement. The acute angled vanes were more in line with the expected characteristics of CS3D and were hence chosen for further studies.

Fig. S15(a)–(c)† in the ESI† show a closer view of the velocity vector and contour profiles of the CS3D geometries. The solute is suspended while moving convectively to the next segment, while the primary solvent permeates through the membrane. Fig. S15(b)† is designed with the same intuition towards mixing and splitting the primary flow; however, the form drag created behind the rectangular obstacle slows down the stream and enhances the back-flow just at the intersection with the dilutant flow which prevents vortex formation and advects the two mixed streams to the next segment. Hydrofocusing occurs on the bottom part of the rectangular obstacle to form a thin lamellae flow and promote stretching and mixing. However, it seems that the bulk of the stream splits and moves over the rectangular obstacle and not under.

In Fig. S15(c),† the mixer is designed to allow the counter current interaction of the two streams. The two streams meet at an angle of 120° and move in stratified layers. There
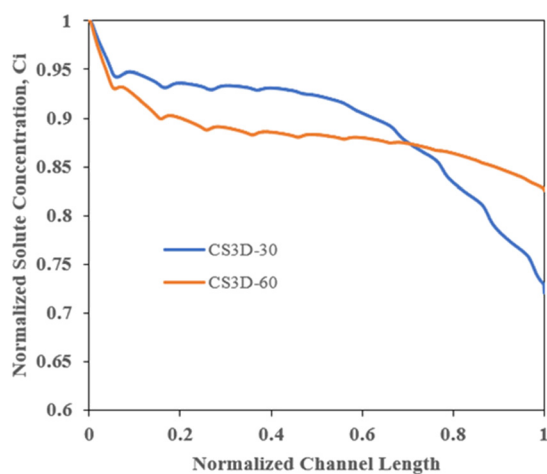
This journal is © The Royal Society of Chemistry 2023

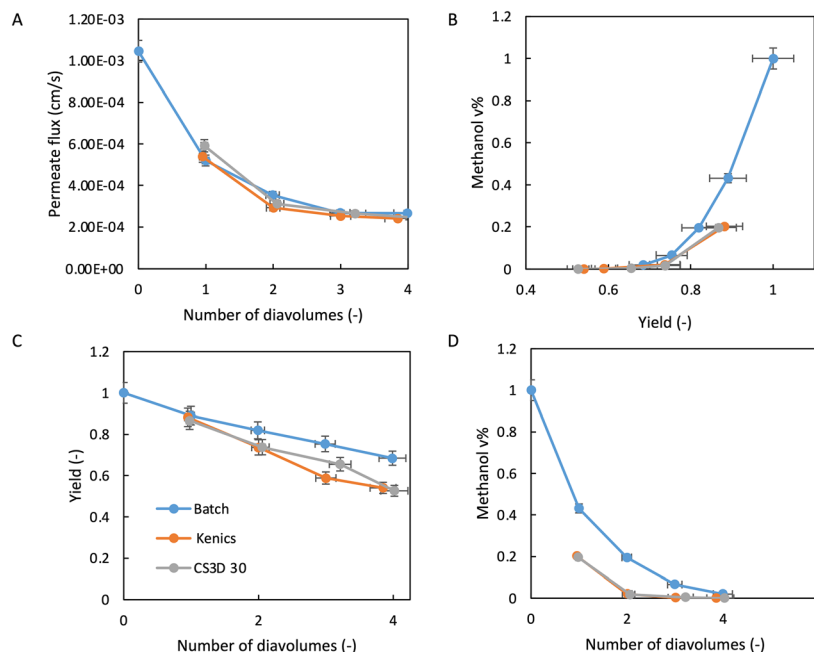*React. Chem. Eng.*, 2023, **8**, 1785–1798 | **1791**

Fig. 8 Performance analysis for CSDD type mixers for solvent exchange: (A) permeate flux (cm s^{-1}) as a function diavolumes utilized, (B) residual methanol% (purity) as a function yield achieved, (C) yield as a function of the number of diavolumes utilized, and (D) residual methanol% (purity) as a function of the number of diavolumes utilized. Mean values are calculated from independent steady state attaining experiments plotted with standard error of the mean (n = 3).

doesn't appear to be much mixing occurring between the two layers in the transverse direction. The primary flow permeates along the channel length and forms a thin layer while the solute API is picked up by the dilutant flow and moves along the channel length. Fig. 5(d)–(g) are representative of the CS3D concept; the buffer flow impinges on the surface of the membrane while the axial flow drives all the components along the membrane channel. Two mixer geometries were fabricated, CS3D 30 and 60, and were experimentally tested to analyze their performance. They have 30 degree and 60 degree impingement angles and CFD simulations are shown in Fig. 4(e) and (g), with photographs of the fabricated parts found in the ESI.† CS3D 45 may have attributes of both mixers; however, analyzing the CS3D 30 and 60 geometries allows us to evaluate closely the extremes of the two effects in acute angle mixers.

4.3 Flow visualization and analysis of CS2D geometries

CS2D type mixers aim to achieve an equivalent purification efficiency in terms of yield and purity as batch diafiltration, while avoiding a reduction in flux associated with increased polarization due to displacement effects. The designs have been inspired by the commonly used Kenics and SMX mixers with further modifications and designs to incorporate the hold-up and compartmentalization of the flow within the channel. A CFD informed design process was used to develop the final mixer that can generate the flow fields required for the CS2D operation while also being compatible with

geometry constraints associated with available 3D printers. Details of which can be found in the ESI.†

In Fig. S16 (ESI†), the rotational influence of the Kenics mixer is observed. This plays a critical role in sweeping off the concentration polarization layer near the membrane interface and in the suspension of the solutes, a key element in the CS2D process. CS2D principally desires such mixing, where the microsolute and macrosolute mix and suspend. The secondary flow brings the stagnating fluid elements from the wall surface to the central bulk of the segment where mixing and homogenizing of the two miscible flows take place. Intuitively radial mixing is not desirable as it leads to fluid stagnation at the walls; however, the mixers are built to promote flow inversion and to stretch and fold fluid blobs until mixing occurs, bringing the fluid in rather than pushing it away to the membrane wall.[32,37]

4.3.1 Downstream vortex formation. The presence of gaps between the mixing elements promotes mixing with fewer elements and a lower pressure drop along the channel length.[32] In the current study with a Kenics type mixer, the spacing between the mixing elements was provided to aid in the additive manufacturing process (ESI† sections 3 and 4). The SMX type mixer in particular shows strong rotational vortices along the length of the flow between the mixing elements (Fig. S18 (ESI†)). The strong rotational flow can be attributed to the mitigation of the concentration of the polarization layer and enhancing the permeation flux besides the extent of dispersive mixing. The spacing between the mixing elements is much pronounced in the case of the SMX

1792 | *React. Chem. Eng.*, 2023, **8**, 1785–1798

This journal is © The Royal Society of Chemistry 2023

mixer to incorporate better mixing and purification characteristics.

Fig. 5 shows the influence of the mixing strategies on the membrane unit for SMX, Kenics and CS3D 45 type mixers. The permeation flow rate increases along the length for the SMX type mixer significantly and the concentration polarization layer decreases simultaneously. The SMX mixer with four mixer segments proves to be more effective against the Kenics type mixer along the length of the channel. The localized mixing in the case of the Kenics type mixer is much higher; however, due to the lack of spacing between the mixing elements for separation to take place, more polarization of the solute at the membrane surface is observed. Similar or greater concentration polarization was observed in the Kenics mixer compared to the CS3D-45 mixer over the first half of the channel length.

5. Results and discussion

5.1 Experimental characterization of CSDD performance

Fig. 6 shows a comparison of the performance in continuous operation for all utilized mixers in addition to semi-batch constant volume diafiltration. The experimental performance of the constant volume batch diafiltration process is outlined in more detail in the ESI† (section 1). Fig. 6A shows the purity achieved in each of the experimental runs as a function of the yield at which it was achieved. This is derived from steady state yields and purities from the operation at feed to diavolume flow rate ratios in the continuous runs of 1:1, 1:2, 1:3 and 1:4. Fig. 6B shows the permeate flux measured in each of the experimental runs as a function of the number of diavolumes utilized. Fig. 6C and D show the yield (eqn (3)) and purity (eqn (4)) of each of these runs as a function of the number of diavolumes added (batch) and the relative feed to diavolume flow rates (continuous).

From Fig. 6, continuous spatially distributed diafiltration has been successfully implemented to provide single-stage solvent efficient continuous purification of the model product-impurity OSN process evaluated in this study. Firstly, in Fig. 6C, the purity achieved in the CSDD runs exhibits an increased efficiency with respect to the number of diavolumes of solvent consumed. This is as would be anticipated based on the conceptual model and washout curves outlined in section 2 and Fig. 2.

The solvent efficiency, as defined as the increase in achieved purity as a function of the number of diavolumes utilized, indicates that there has been displacement of feed crossflow by orthogonal diavolume flows with only partial mixing, (*i.e.* displacement effects). As would be anticipated from the simple CS2D/CS3D conceptual models, outlined in section 2, a number of the continuous mixers (Kenics, CS3D60) show a reduction in permeate flux compared to the equivalent batch diafiltration (Fig. 6B). However, several mixer configurations were successful in avoiding any observed reduction in average flux, in spite of improved purification as a function of diafiltration solvent

consumption (Fig. 6C). As can be seen in Fig. 5, each static mixing element incrementally reduces concentration at the membrane interface and improves flux along the length of the channel, negating or in the case of the SMX mixer reversing expected reductions in flux. It should be noted that this is in comparison to a simple laminar channel-based batch diafiltration, and increased or equivalent flux would not be anticipated in runs at the same improved diafiltration solvent efficiency if significant turbulence or effective membrane channel laminar mixing strategies were to be employed in batch operation.[33]

The overall results presented in Fig. 6 broadly correspond to the proposed simple conceptual model outlined in section 2, for the relative effect of mixedness in the transmembrane direction and associated displacement effects on diafiltration efficiency. However, this conceptual model does not suggest what effect the continuous spatially distributed diafiltration should have on purification efficiency, as defined as the observed relationship between yield and purity shown in Fig. 6A. This motivated the selection of the experimental system used in this study where quantitative product rejection is not achieved and non-zero rejection of impurity occurs. In Fig. 6A, each of the mixers utilized in continuous operation shows equivalent or greater purification efficiency for this non-ideal membrane separation in comparison to the equivalent constant volume batch diafiltration. Furthermore, the Kenics mixer and CS3D-30 mixer provide a significant improvement in terms of performance in this respect. For example, with the addition of 4 diavolumes under equivalent conditions, the Kenics mixer runs achieved a yield of 65% and purity of 77%, and the CS3D-30 mixer runs achieved a yield of 63% and purity of 74%, compared to the batch diafiltration which achieved a yield of 60% and a purity of 55%. This implies that concentration polarization, resulting from displacement effects, occurring along the membrane channel has an asymmetric and beneficial effect on the observed rejection of the product (ibuprofen) compared to the impurity (ethanol), as they will both undergo displacement towards the membrane interface within the channel but with the alternate local concentration at the membrane interface resulting in an asymmetric change in observed rejection across the CSDD mixer and batch configurations.

This improvement in purification efficiency (Fig. 6A) will be dependent on the chemical composition of the system (products, impurities, solvents), the physicochemical properties in solution, the characteristics of the membrane, the flow field, the concentration field, and the interaction between these parameters. Hence, it will require further investigation with a wide range of experimental product-impurity and solvent systems with a wide array of membrane materials and MWCOs to ascertain how frequently improvements in purification or the reverse will occur with the CSDD operation for non-ideal membrane separations. It should be noted that rejection is often calculated using the formula shown in eqn (12) (ESI†), which is based on the

This journal is © The Royal Society of Chemistry 2023

React. Chem. Eng., 2023, **8**, 1785–1798 | 1793

average performance for a membrane module, and this may be sufficient for batch or continuous CSTR type mixed membrane diafiltrations; however, observed rejection is likely to be spatially varying in real CSDD experiments as interface concentration and flux can vary significantly across the membrane channel as seen in CFD simulations in Fig. 5.

From a process intensification, efficiency, operational and green chemistry standpoint, the results indicate that CSDD may present an attractive alternative to currently utilized batch and continuous membrane diafiltration strategies for purification of process streams. Firstly, operationally, CSDD provides a viable solvent efficient single stage diafiltration operation ideal for in-line purification in continuous chemical or continuous biopharmaceutical production that can likely be applied to other challenges in the process industries. This eliminates the need for buffer tanks and control required by parallel batch diafiltration or interstage pumps and multiple units required in continuous counter-current cascades that are challenging to implement at small scales of inflow chemical or process development environments. CSDD operation is also more productive than batch operation which may yield further improvements in capital costs due to a reduced equipment scale.

As outlined in the Introduction (section 1), continuous processes are increasingly employed in the synthesis of complex high value chemical products that typically require a significant number of synthetic steps between which there is a need for purification and conditioning of intermediate streams. The improved yield (Fig. 6A) that has been attained in the CS3D-30 and Kenics mixer runs would be of significant utility in such processes where specialized intermediates and API products can be highly valuable. The ability to conduct single phase purification of process streams to purge salts, reagents, impurities, and exchange process solvents is a key requirement that currently limits solvent selection due to the requirement to enable intermediate liquid–liquid extractions as the preferred intermediate purification step in flow chemical operations to currently provide this functionality. In such applications, the molecular weight of intermediates will most often increase throughout the synthesis. Therefore, membrane separations if employed would be most often required to retain the highest molecular weight species as in the example model system utilized here. However, this is not always the case and high molecular weight–high-cost catalyst complexes and enzymatic catalysts of greater molecular weight compared to process intermediates also must be removed from process streams. Convenient semi-permeable continuous membrane separation operations would enable homogeneous catalyst separation and direct reuse that is often forgone in batch operation with the intermediate being removed in the permeate stream from the membrane.[29] The higher solvent efficiency of CSDD (Fig. 6C and 8D), in addition to improving processes efficiency, would have an additional benefit of more concentrated permeate process streams in these examples. In such cases, the need for subsequent concentration of intermediate containing

permeate streams may be mitigated or eliminated therefore providing an additional possible attraction of the approach for continuous chemical applications.

Solvent requirements are reduced significantly compared to batch operation, a key goal in terms of development of green processes, in addition to reducing operational costs. This directly reduces energy requirements also in solvent recovery/disposal and in pumping through the membrane owing to reduced total permeation requirements at equivalent or even improved flux (Fig. 6). This may be considered to be partially offset by the increased retentate side pressure drop occurring due to the presence of the mixer elements; however, in most cases, the back pressure placed on the system to drive permeation will be far more than the pressure drop induced by the mixer. While CSDD mixers with improved or equivalent flux to batch operation were demonstrated (Fig. 6) this may be offset or reversed with the application of turbulence promoting mixers in batch operation, so strong conclusions about improvement in energy efficiency in the industrial application of CSDD as a result of improved flux cannot be made without further investigation. Solvent requirements may be reduced further by employing CSDD in a counter current cascade configuration which will also have a further positive impact on the process yield at a specified level of stream purity for imperfect membrane separations.

5.2 CFD and experimental analysis of deviation of real CSDD purification results from idealized CS2D/CS3D performance

The results in section 5.1 indicate that the primary objectives of continuous spatially distributed diafiltration have been achieved with single stage operation demonstrated to achieve similar or improved purification efficiency and reduced diafiltration solvent requirements compared to the equivalent batch separation. These results also broadly correspond to the proposed simplified conceptual model outlined in section 2, for the relative effect of mixedness in the transmembrane direction and associated displacement effects on diafiltration efficiency. However, this conceptual model is an oversimplification of the complex spatially non-uniform velocity and concentration fields and their interaction with the observed membrane separation within the continuous mixer experiments. This limitation of the conceptual model manifests in the divergence between observed permeate flux in the CS3D-30 mixer at similar levels of purification efficiency to the Kenics mixer, which improves upon batch purification without an observed reduction in permeate flux. Additionally, the idealized conceptual model cannot provide a ready explanation for the combination of reduced purification efficiency and reduced flux observed in the experimental runs for the CS3D 60 mixer compared to the CS3D 30 variant. For this reason, the CFD analysis used in the design of these mixers outlined in detail in section 4 is applied to these cases to further elucidate the continuous spatially distributed diafiltration operation in these cases.

The CS3D-30 and Kenics type mixers both outperform the batch significantly in terms of purification efficiency, with this difference increasing with increasing diafiltration ratios for both mixers as observed from the experiments (Fig. 6A). However, the CS3D-30 runs when compared to the batch diafiltration data do not exhibit a significant reduction in permeate flux (Fig. 6B). It is suspected that this may be because the buffer entry in CS3D-30 is more tangential to the main channel flow resulting in an acceleration of the flow at the membrane surface and a more stratified concentration profile near the membrane (Fig. S19, ESI†). There are two reasons that may account for the reduced permeate flux in the Kenics mixer from the CFD simulations: (1) strong localized mixing because of the mixer geometry and hence an incomplete forward movement of the solution in the crossflow direction and (2) the lack of spacing between the mixer segments which results in improper diafiltration dilution with the buffer. For CS3D-30, the displacement effects are similar relative to the Kenics type mixer based on observed purification efficiency trends (Fig. 6A), but the Kenics mixers exhibit stronger local mixing of the solute and higher local polarization.

The CS3D type mixers are intrinsically designed with displacement effects when compared to the CS2D type mixers. The CS3D mixers with two different vane angles (30° and 60°) were tested experimentally with CS3D-60, having both lower permeate flux and purification efficiency compared to the CS3D 30 mixer runs under tested conditions (Fig. 6). For the CS3D-60 mixer, the effective permeation flux as observed in Fig. 6(b) is much lower than that of batch diafiltration, which is 25% higher.

Fig. S19† shows a comparison of the solute concentration at the intersection of the top inlet and the bulk flow along the membrane channel. Convective effects in the crossflow direction at the membrane interface are more pronounced in the case of CS3D-60. The secondary buffer in CS3D-60 enters the channel region (nearly) perpendicular to the channel length; however, it doesn't have a strong displacing effect. The secondary buffer fluid adds to the momentum of the bulk flow and contributes to the crossflow. The fast-moving fluid flow close to the membrane surface increases above the local permeation that can displace through the membrane, creating a net bypassing effect (Fig. S20, ESI†).

The buffer entry in CS3D-30 is more tangential to the main channel flow relative to that observed in CS3D-60. At the point of intersection, the main channel feed and the entering buffer feed combine in a faster moving flow which results in reduced localized pressure. This resulting drop in pressure creates an upswell which is strongly observed in CS3D-30 relative to CS3D-60. Notable observations at (or near) the membrane surface for CS3D-30 relative to CS3D-60 are (a) reduced flow velocity at (or near) the membrane surface, 7.86% lower in CS3D-30; (b) greater stratification of the solute concentration; (c) a displacement effect followed by a relieving pressure at the points of intersection of the two feeds, acceleration followed by deceleration.

The higher residence time of the solute in CS3D-30 contributes to its higher level of displacement and observed purification efficiency. Fig. 7 shows the predicted solute concentration at the membrane interface in CS3D-30 against CS3D-60 using CFD. For the first 75% of the channel length, CS3D-30 is observed to have higher solute concentration at the membrane interface due to the stronger displacement effects and reduced permeation flux (Fig. 6(B)) present relative to CS3D-60. For the remaining 25% of the channel length, the steep angled inlets of the buffer flow in CS3D-30 result in a washout of the solute resulting in better average yields (Fig. 6(A)). Overall analysis of the CFD simulations corresponding to these runs indicate that higher solute hold-up at the membrane interface and thinner layers of stratification drive the improved CS3D-30 performance in terms of both purification efficiency and flux in comparison to the CS3D-60 mixer experiments.

5.3 Towards idealized CS2D performance in real CSDD mixers

With respect to the CS2D inspired mixer designs (sections 2 and 4.3), the Kenics type mixer shows a significant enhancement in purification efficiency compared to the serpentine and SMX type mixers, which both show similar performance to batch diafiltration efficiency (Fig. 6A). The Kenics type mixer achieved a 17% higher yield with a 9.9% higher product purity compared to the SMX type mixer at 4 diavolumes of the relative flow rate to that of the feed. However, the performance of the Kenics type mixer converges with that of the SMX as the diavolume flow rate ratio reduces to 1:1. The improved relative performance in terms of purification efficiency suggests that the Kenics mixer is less efficient at transporting solutes away from the membrane fluid interface, opposite to the diavolume flows in the transmembrane direction. Therefore, resulting in less crossflow/diavolume flow mixing and greater displacement effects, resulting in lower permeate flux as per Fig. 6B but enabling a higher diafiltration solvent efficiency in reaching a desired purity set point (Fig. 6C).

CFD simulations show that the SMX type mixer created strong flow recirculation along the length of the membrane channel (Fig. S18†) which contributes to the lower concentration at the membrane surface (Fig. 5) and hence higher permeate flux (Fig. 6B). The SMX type mixer had 21% higher permeate flux compared to Kenics. The Kenics type mixer has 12% lower flux than batch at 4 diavolumes of relative flow rates. The SMX mixer however in contrast to the Kenics mixer only demonstrated equivalent or minor improvement in purification efficiency compared to batch operation across the range of conditions tested (Fig. 6A). Although at a lower relative diavolume flow rate of 1:1 in place of 1:4 (Fig. 6B), the purification efficiency of the two continuous mixer experiments converged with equivalent or marginal performance improvements in purification efficiency in comparison with the batch operation at this

This journal is © The Royal Society of Chemistry 2023

React. Chem. Eng., 2023, **8**, 1785–1798 | **1795**

point. The SMX mixer performance is equivalent to that of batch diafiltration in terms of purification efficiency (Fig. 6A).

However, based on the improved solvent diafiltration consumption at all purity values (Fig. 6C), even the SMX mixer with the highest efficiency and flux observed has failed to approximate the idealized CS2D operation as outlined in section 2. Although real mixer performance approximating idealized CS2D (section 2) will have reduced efficiency in terms of diafiltration solvent requirements and purification efficiency compared to that demonstrated in this study, it will be desirable for conducting continuous spatially distributed diafiltration for systems that have large reductions in permeability when concentration polarization occurs or where membrane fouling or solute precipitation are concerns that warrant limiting the concentration within the membrane system. Experimentally, this should be observed when the diafiltration solvent efficiency for purification shown in Fig. 6C reduces to that of an equivalent batch diafiltration with good mixing characteristics. This can be achieved in a laminar flow environment by adding more static mixing elements per unit of residence time within the membrane channel. The ability to do this within this study was limited by the smallest feature sizes available for fabrication of the SMX and Kenics mixers *via* 3D printing and should be easier to achieve in larger membrane systems, although further experimental and computational optimization will be required to this end. Highly turbulent flows where achievable may approach such flow profiles also where they can be harnessed.

5.4 Continuous spatially diafiltration for in-line solvent exchange processes

Section 5.1 demonstrates a proof of concept for the use of continuous spatially distributed diafiltration for the purpose of efficient single stage continuous diafiltration for stream purification. In Fig. 8, the CS3D-30 and Kenics mixers that were found to have the highest efficiency in terms of diafiltration solvent utilization (Fig. 6C) and purification efficiency (Fig. 6A) are used to conduct solvent exchange as per the experimental procedure outlined in section 3.4, switching ibuprofen as the model product from an inlet methanol solution to an outlet solvent ethanol solution. The single step, single module, single phase continuous solvent exchange process that could be offered by CSDD would represent an extremely useful stream adjustment technique for multi-step integrated flow chemical processes and automated experimentation. Similarly, the equivalent aqueous buffer exchange operation would be of high utility for stream adjustment in continuous biopharmaceutical downstream operations.

Fig. 8 presents the experimental results for CSDD solvent exchange runs which are again compared to the equivalent constant volume batch diafiltration. Fig. 8A shows the permeate flux for the three runs. From these data, the permeate flux decreases as a function of the number of diavolumes utilized in both batch and continuous operations, as methanol is replaced as the continuous solvent phase by ethanol. The CSDD operations exhibit an equivalent slightly increased flux when operating at 1 diavolume of relative flow (Kenics 3.6%, CS3D30 13.6%) compared to the batch operation with an equivalent or slightly reduced flux compared to batch at diavolumes of 2 (Kenics 17%, CS3D30 12%), or above.

Fig. 8B presents the purification efficiency for the process, in this case defined as process yield as a function of the remaining fraction of methanol in the outlet stream. The purification efficiency plot (Fig. 8B) is derived from the yield and methanol% data plotted as a function of the number of diavolumes utilized shown in Fig. 8C and D, respectively. Fig. 8B shows that as per section 4.3 the continuous spatially distributed diafiltration operations with the Kenics and CS3D mixers had higher yields than batch diafiltration at all observed levels of purity measured. Fig. 8D shows that the continuous experiments show roughly equivalent levels of diafiltration solvent efficiency to each other in performing the solvent exchange with both showing a far more rapid decrease in methanol retentate outlet percentage as a function of the number of diavolumes utilized than the batch operation. While the yield also decreases at a faster rate in terms of diavolume consumption than that of the batch operation (Fig. 8C), there is no trade-off to be made in terms of product yield and purification efficiency, as both CSDD operations both show enhanced yield at all measured outlet stream specifications for the purity/methanol fraction. At diavolumes amounts of 2 and above, there is a slightly higher flux observed in the batch operation. However, any productivity increases due to flux in batch is more than offset by the need to use significantly increased volumes of the diafiltration solvent to achieve the same outlet purity, which also results in reduced product yield.

Taking the example of the methanol to ethanol stream adjustment targeting 2% residual methanol in the retentate, at approximately a 2 diavolume flow rate relative to the feed flow, this stream purification specification is met by the CSDD operations. The CS3D30 mixer achieves a residual methanol fraction of 1.8% at a corresponding yield of 74%, and the Kenics mixer achieves a residual methanol fraction of 2.1% at a corresponding yield of 74%. At 2 diavolumes of solvent usage in batch diafiltration, the residual methanol fraction is 20%, approximately 10 times higher than the figure achieved in the continuous experiments. The batch diafiltration does not hit a 2% residual methanol endpoint until an addition of 4 diavolumes of ethanol is made, reaching a methanol fraction of 2% at a yield of 69%. Therefore, requiring approximately double the amount of diafiltration solvent to reach the 2% specification for the output purity of this membrane operation and incurring lower yield than the equivalent continuous spatially distributed diafiltration operation in the case of this non-quantitative membrane separation. Where further

1796 | *React. Chem. Eng.*, 2023, **8**, 1785–1798

This journal is © The Royal Society of Chemistry 2023

improvements in solvent consumption and yield are required as with other membrane operations, multiple CSDD units could be arranged in a cascade configuration. At this 2% residual methanol specification, the continuous mixing runs show an increase in productivity of 75% (Kenics) and 92% (CS2D-30) compared to the batch operation. Intensified productivity reduces the equipment footprint on-scale compared to batch. Additionally, equipment requirements are reduced also by removing the intermediate hold tanks to conduct parallel batch diafiltration within continuous operation.

As discussed in section 5.1, additional green metrics for the efficiency of the operation such as specific energy consumption are also likely to be favourable when considering the continuous spatially distributed diafiltration compared to batch diafiltration in industrial application based on the solvent exchange data in Fig. 8. As such, the inclusion of CSDD mixers is unlikely to create significant downside in energy consumption requirements let alone offset improvements in solvent usage efficiency and purification efficiency found with the model experimental system investigated here.

Conclusions

The present work has established a novel mode of continuous diafiltration namely continuous spatially distributed diafiltration by modifying the flow behaviour inside a membrane channel with the help of inline mixers and directional flow distribution. Mixer designs were inspired by two idealized extremes of mixing of the crossflow and orthogonal diavolume flows, CS2D and CS3D, with perfect mixing and non-mixing in these respective directions with idealized flat velocity profiles along the length of the membrane channel. A region of performance was proposed with respect to solvent consumption, with the lower performance limit being that of a batch constant volume diafiltration and the upper performance limit being that of a theoretical displacement with a single diavolume. Concentration polarization is expected to increase as the upper limit and ideal displacement behaviour are approached. The CS2D mixer was expected to behave closer to batch whereas CS3D was closer to the ideal displacement behaviour.

A model chemical system and OSN membrane were utilized within a rectangular membrane channel modified to be able to include 3D printed mixers to distribute continuous spatially introduced diavolume flows in order to approach or approximate the idealized CS2D and CS3D flow regimes envisioned. These experiments proved successful in demonstrating the utility of continuous steady state spatially distributed diafiltration to firstly provide single stage continuous diafiltration operation and furthermore a significant scope for improved solvent consumption efficiency compared to batch operation. Finally, improvements in yield as a function of target purity could

also be realized *via* this approach in comparison to the equivalent batch diafiltration operation. No trade-offs in terms of productivity, energy consumption or other process metrics were required, with CSDD meeting or exceeding the performance of the equivalent batch diafiltration. In systems prone to membrane fouling or product precipitation, a trade-off between improved solvent efficiency resulting from mixers with increased displacement effects and increased polarization resulting in more rapid membrane fouling is likely to occur and will require further investigation.

It should be noted that these mixers are by no means the fully optimum attainable configuration and are presented as a proof of concept for this new mode of diafiltration within this study. As such mixers with improved trade-offs between flux, solvent efficiency, and purification efficiency and retentate side pressure drop may be found. Furthermore, the performance of this model chemical and membrane system combination does not imply that this membrane will be suitable for solvent switching for all solvent and chemical system combinations, as additional membrane screening will be required for specific systems.

The approach should be readily scalable with a significant scope to lengthen/broaden the channel and also number up. The approach should be extendable to alternate channel geometries, for example spiral wound and tubular configurations for further scale-up. The approach is also highly suited for scale-down automated experimentation and microfluidic applications as laminar mixing can be initiated at very small scales as long as flow rates over laminar mixers are sufficiently fast where the timescales for convection in the transmembrane direction remain significantly faster than diffusion timescales.

Author contributions

Zoheb Khan: software, investigation, validation, formal analysis, writing-original draft, visualization, and writing-review and editing. Xiaoyan Long: investigation, validation, writing-original draft, and writing- review and editing. Eoin Casey: funding acquisition. Denis Dowling: resources. Steven Ferguson: conceptualization, methodology, supervision, writing-original draft, writing- review and editing, visualization, project administration, and funding acquisition.

Conflicts of interest

There are no conflicts to declare.

Acknowledgements

This journal is © The Royal Society of Chemistry 2023

React. Chem. Eng., 2023, **8**, 1785–1798 | 1797

References

1 A. Adamo, R. L. Beingessner, M. Behnam, J. Chen, T. F. Jamison, K. F. Jensen, J. C. M. Monbaliu, A. S. Myerson, E. M. Revalor, D. R. Snead, T. Stelzer, N. Weeranoppanan, S. Y. Wong and P. Zhang, *Science*, 2016, **80**, 352.

2 S. Mascia, P. L. Heider, H. Zhang, R. Lakerveld, B. Benyahia, P. I. Barton, R. D. Braatz, C. L. Cooney, J. M. Evans, T. F. Jamison, K. F. Jensen, A. S. Myerson and B. L. Trout, *Angew. Chem., Int. Ed.*, 2013, **52**, 12359.

3 M. A. Sciberras and G. N. Coleman, *Eur. J. Mech. B Fluids*, 2007, **26**, 551.

4 K. P. Cole, B. J. Reizman, M. Hess, J. M. Groh, M. E. Laurila, R. F. Cope, B. M. Campbell, M. B. Forst, J. L. Burt, T. D. Maloney, M. D. Johnson, D. Mitchell, C. S. Polster, A. W. Mitra, M. Boukerche, E. W. Conder, T. M. Braden, R. D. Miller, M. R. Heller, J. L. Phillips and J. R. Howell, *Org. Process Res. Dev.*, 2019, **23**, 858.

5 R. Godawat, K. Konstantinov, M. Rohani and V. Warikoo, *J. Biotechnol.*, 2015, **213**, 13.

6 I. R. Baxendale, R. D. Braatz, B. K. Hodnett, K. F. Jensen, M. D. Johnson, P. Sharratt, J. P. Sherlock and A. J. Florence, *J. Pharm. Sci.*, 2015, **104**, 781–791.

7 A. Weeranoppanant and N. Adamo, *ACS Med. Chem. Lett.*, 2019, **11**, 9–15.

8 T. F. Jamison, Separation and Purification in the Continuous Synthesis of Fine Chemicals and Pharmaceuticals, *Flow Chem. Org. Synth.*, 2018, ch. 3, vol. 5.

9 L. Gerstweiler, J. Bi and A. P. J. Middelberg, *Chem. Eng. Sci.*, 2021, **231**, 116272.

10 P. Marchetti, L. Peeva and A. Livingston, *Annu. Rev. Chem. Biomol. Eng.*, 2017, **8**, 473.

11 D. J. Gravert and K. D. Janda, *Chem. Rev.*, 1997, **97**, 489–510.

12 L. Peeva, J. da Silva Burgal, I. Valtcheva and A. G. Livingston, *Chem. Eng. Sci.*, 2014, **116**, 183.

13 D. Vogelsang, J. M. Dreimann, D. Wenzel, L. Peeva, J. da Silva Burgal, A. G. Livingston, A. Behr and A. J. Vorholt, *Ind. Eng. Chem. Res.*, 2017, **56**, 13634.

14 P. Kisszekelyi, A. Alammar, J. Kupai, P. Huszthy, J. Barabas, T. Holtzl, L. Szente, C. Bawn, R. Adams and G. Szekely, *J. Catal.*, 2019, **371**, 255.

15 L. Peeva, J. Da Silva Burgal, Z. Heckenast, F. Brazy, F. Cazenave and A. Livingston, *Angew. Chem.*, 2016, **128**, 13774.

16 S. So, L. G. Peeva, E. W. Tate, R. J. Leatherbarrow and A. G. Livingston, *Org. Process Res. Dev.*, 2010, **14**, 1313.

17 R. Dong, R. Liu, P. R. Gaffney, M. Schaepertoens, P. Marchetti, C. M. Williams, R. Chen and A. G. Livingston, *Nat. Chem.*, 2019, **11**, 136.

18 J. F. Kim, P. R. J. Gaffney, I. B. Valtcheva, G. Williams, A. M. Buswell, M. S. Anson and A. G. Livingston, *Org. Process Res. Dev.*, 2016, **20**, 1439.

19 V. Voros, E. Drioli, C. Fonte and G. Szekely, *ACS Sustainable Chem. Eng.*, 2019, **7**, 18444.

20 E. Rundquist, C. Pink, E. Vilminot and A. Livingston, *J. Chromatogr. A*, 2012, **1229**, 156.

21 S. Ferguson, F. Ortner, J. Quon, L. Peeva, A. Livingston, B. L. Trout and A. S. Myerson, *Cryst. Growth Des.*, 2014, **14**, 617.

22 T. Renouard, A. Lejeune and M. Rabiller-Baudry, *Sep. Purif. Technol.*, 2018, **194**, 111.

23 A. Lejeune, M. Rabiller-Baudry and T. Renouard, *Sep. Purif. Technol.*, 2018, **195**, 339.

24 A. Jungbauer, *Trends Biotechnol.*, 2013, **31**, 479.

25 A. L. Zydney, *Biotechnol. Bioeng.*, 2016, **113**, 465.

26 C. Casey, T. Gallos, Y. Alekseev, E. Ayturk and S. Pearl, *J. Membr. Sci.*, 2011, **384**, 82.

27 A. Arunkumar, N. Singh, M. Peck, M. C. Borys and Z. J. Li, *J. Membr. Sci.*, 2017, **524**, 20–32.

28 R. Tan, F. Hezel and M. Franzreb, *J. Membr. Sci.*, 2021, **619**, 118695.

29 P. Marchetti, M. F. J. Solomon, G. Szekely and A. G. Livingston, *Chem. Rev.*, 2014, **114**, 10735.

30 A. L. Zydney, *Curr. Opin. Chem. Eng.*, 2015, **10**, 8.

31 P. A. Tanguy, L. Fradette, M. Heniche and S. A. Jaffer, *CFD Simulations of Static Mixers: A Survey, Mixing and Compounding of Polymers*, Carl Hanser Verlag GmbH & Co. KG, 2009, ch. 9.

32 B. W. Nyande, K. M. Thomas and R. Lakerveld, *Ind. Eng. Chem. Res.*, 2021, **60**, 5264.

33 K. Y. Toh, Y. Y. Liang, W. J. Lau and G. A. F. Weihs, *Membranes*, 2020, **10**, 10.

34 F. Xie, H. Ge, J. Liu, W. Chen and H. Song, *Chem. Eng. Process.*, 2018, **127**, 28.

35 B. Sutariya, A. Sargaonkar, B. K. Markam and H. Raval, *Chem. Eng. J. Adv.*, 2022, **11**, 100335.

36 A. Parvareh, M. Rahimi, S. S. Madaeni and A. A. Alsairafi, *Chin. J. Chem. Eng.*, 2011, **19**, 18.

37 M. M. Haddadi, S. H. Hosseini, D. Rashtchian and M. Olazar, *Chin. J. Chem. Eng.*, 2020, **28**, 672.

38 S. Ahmed, M. Taif Seraji, J. Jahedi and M. A. Hashib, *Desalination*, 2011, **276**, 191.

39 M. J. Harding, S. Brady, H. O'Connor, R. Lopez-Rodriguez, M. D. Edwards, S. Tracy, D. D. Dowling, G. Gibson, K. P. Girard and S. Ferguson, *React. Chem. Eng.*, 2020, **5**, 728.

40 A. L. Ahmad and K. K. Lau, *Ind. Eng. Chem. Res.*, 2007, **46**, 1316.